Regular Paper ISSN- 0102-9010

MORPHOMETRIC ANALYSIS OF THE FATE OF SECRETORY EPITHELIAL CELLS IN THE VENTRAL LOBE OF THE RAT PROSTATE DURING MASSIVE APOPTOSIS

Eduardo Albert Frankfurt*, Teng Chang Li, Michael Jenwei Chen, Marcelo A. Ferreira, Joyce T. Kawakami, Karina Silva Funabashi, Maria Fernanda Malvezzi and Antonio Sesso

Sector of Structural Biology , Laboratory of Immunopathology, Institute of Tropical Medicine, University of São Paulo (USP), São Paulo, SP, Brazil.

ABSTRACT

Orchiectomy causes marked, rapid involution of the prostatic secretory epithelium. Concurrently, macrophages, which in normal glands are small and rarely occur at the base of the secretory epithelium, increase in size and number. Apoptotic cells are engulfed by companion epithelial cells and also by macrophages. In secretory cells and macrophages, dense bodies progressively increase in number and store membranes derived from dead cells of the secretory epithelium. In this work, we examined the contributions of the various routes of disposal of demised secretory epithelial cells of the rat prostate, induced to enter in apoptosis by retrieval of androgen. Specifically, we sought to determine how much membrane surface area derived from apoptotic cells of the secretory epithelium could be stored in dense bodies, and how these data compared with the disposal of dead cells via the glandular lumen. Glands from unoperated controls (day 0) and from rats examined 12 h and 1, 2, 3, 4, 5, 6, 7, 8, and 9 days after orchiectomy were studied morphometrically. The total membrane surface area of rough and smooth endoplasmic reticulum, Golgi apparatus, mitochondria and vesicles declined from 6.75×10^3 μm^2 in non-castrated rats to 1.12×10^3 μm^2 nine days after castration. Similarly, the total surface area of the secretory epithelium decreased from 10.6×10^{11} μm^2 in non-castrated rats to 0.204×10^{11} μm^2 nine days after castration. Geometrical models revealed that 1 μm^3 of dense body accommodated at least 142 μm^2 of myelin-like membrane surface area. Three to four days after castration, the total volume of intramacrophage dense bodies peaked ($\sim 5 \times 10^6$ μm^3) and represented 1-2% of the volume of intraepithelial dense bodies ($\sim 4 \times 10^8$ μm^3). The minimum membrane surface area that could be stored in dense bodies of the secretory epithelium on post-castration days 0, 1, 2, 3, 4 and 9 was 1.4%, 9%, 16%, 23%, 28% and 44%, respectively, of the total membrane surface area of the secretory epithelium. The total number of cells counted in the glandular lumina on days 4 and 5 represented 2.6% and 1.2% of the number of cells lost in the glands between post-castration days 3 and 4 and days 4 and 5, respectively. As stated, a relevant source of cell disposal is represented by the autophagic process which occurs in the secretory epithelial cells and results in the formation of dense bodies. Digestion of remnants of apoptotic secretory epithelial cells in the cytoplasm of macrophages and removal of dead cells via the intraluminal route accounted for some 1-3 to 3-4 % , respectively, of the total cell death.

Key words: Apoptosis, castration, dense bodies, electron microscopy, macrophages, morphometry, prostate

INTRODUCTION

The rat prostate consists of three lobes, each with a peculiar acinar pattern and varying sensitivities to testicular hormones [2,3,4,13,18]. These lobes are referred to as ventral, lateral and dorsal based on their position relative to the urethra. The lateral and dorsal lobes are structurally more related to each other than to the ventral lobe [16,20]. TUNEL labeling has revealed apoptosis in the ventral lobe of castrated rats, with the peak number of apoptotic cells occurring on the third day after castration; in the lateral lobe, the peak apoptotic response occurs 3-6 days after castration, while in the dorsal lobe the maximum effect occurs on the sixth day after castration [20]. Transmission electron microscopy (TEM) studies of the structural effects of castration

Correspondence to: Prof. Antônio Sesso
Laboratório de Imunopatologia da Esquistossomose (LIM-06), Setor de Biologia Estrutural, Instituto de Medicina Tropical (IMT), Universidade de São Paulo (USP), Prédio II, 2º andar, Av. Dr. Enéas de Carvalho Aguiar, 500, CEP 05403-000, São Paulo, SP, Brazil. Tel. (55) (11) 3066-7061 and 3061-0707, Fax (55) (11) 3064-5132. E-mail: antses88@uol.com.br

*This work was presented by Eduardo Albert Frankfurt (1962-2005) to the Faculty of Medicine of the University of São Paulo in 2000 as partial fulfillment of the requirements for the degree of Medical Doctor.

on the secretory epithelium of the ventral lobe of the rat prostate [6,12,14,15] were reported prior to the finding that apoptosis was the causative agent of epithelial involution [17].

In different strains of rat, TEM has shown that orchiectomy causes a marked reduction in the secretory epithelium of the prostatic ventral lobe. By day 10 after castration, the cells are reduced to less than half of their original height. This reduction is accompanied by atrophy of the cytoplasm and an epithelial infiltration of macrophages at the base of the secretory epithelium 2-3 days after castration. In these initial days after castration, the rough endoplasmic reticulum (RER) appears as a well-developed system of channels permeating the entire cell. On day 2 post-castration, the cisternae often show a concentric arrangement, forming spheres of RER that are accentuated in the supranuclear region [6,12,14,15,20]. In this cytoplasmic region, membranous whorls and autophagic vacuoles appear, with the latter being bordered by one or two smooth-surfaced membranes. The autophagic digestion of various sized vacuoles gives rise to dense residual bodies and to lipofuscin-like granules that accumulate in the cytoplasm [14]. There is also an increase in the number of macrophages observed phagocytizing such structures [15].

In 1973, Kerr and Searle [17] reported an extensive loss of rat prostatic gland epithelial cells as a result of enhanced apoptosis following orchiectomy. Apoptotic bodies derived from epithelial cells were phagocytized by macrophages scattered along the epithelial surface of the acinar basement membrane. The cytoplasm of these macrophages extended towards the lumen between epithelial cells. The authors expressed the opinion that the macrophages did not increase in number but, instead, became more noticeable because of their enlarged cytoplasm that was filled with residual bodies.

TEM of prostatic tissue from castrated rats has shown that the dense bodies present in the cytoplasm of secretory epithelial cells and macrophages originate from the compaction of membranes derived from various organelles of apoptotic epithelial secretory cells. In macrophages, these dense bodies derive from previously phagocytized spheroidal cytoplasmic portions of apoptotic secretory epithelial cells. These findings indicate that variable amounts of apoptotic cells, apoptotic nuclei and cellular debris are released into the lumen of the glandular units. Using a simple geometrical model, it was possible to estimate the minimum amount of membranous material that could be stored in a unit volume of dense body.

Based on these observations, we have investigated the amount of membrane surface area that can be stored in dense bodies in macrophages and in the cytoplasm of secretory epithelial cells in a given period after orchiectomy. These data were compared with the concomitant decrease in the total membrane surface area (smooth and rough ER, Golgi membranes, mitochondria, vesicles) of the secretory epithelium. The presence apoptotic cells in the acinar lumen was also investigated quantitatively. The number of secretory cells released into acinar lumina was compared with the reduction in the number of these cells in the gland during the previous 24 h.

MATERIAL AND METHODS

Induction of apoptosis

Apoptosis in the secretory epithelium of the prostatic ventral lobe of adult rats weighing 200-300 g was induced by orchiectomy [19]. The ventral lobes from unoperated (control) rats and from castrated rats (1, 2, 3, 4, 5, 6, 7, 8, 9, and 10 days after castration), were desiccated, weighed, fragmented and processed for microscopical analysis. The number of rats varied from 56 for the initial evaluation of the effects of castration on glandular mass, to 16 and 17 rats in other experiments. In general, 16 rats were used, with one rat being examined 12 h and 1, 2 and 3 days after castration, and four rats at day zero and on days 4 and 9 post-orchiectomy.

Light and transmission electron microscopy

For electron microscopy, fragments of prostatic ventral lobe (~1 mm^3) were removed from castrated rats immediately after death, immersed in cold 1.5% glutaraldehyde and 1% paraformaldehyde in 0.08 M cacodylate buffer, pH 7.3, for 2 h, and then washed and stored overnight in this buffer without fixative. The tissues were subsequently post-fixed in one volume of aqueous 2% osmium tetroxide and the same volume of aqueous 3% potassium ferricyanide in 0.08 M cacodylate buffer, pH 7.4, for 2 h, followed by washing in physiological saline and staining en bloc overnight in aqueous uranyl acetate (0.5% water and 106 mg of sucrose per ml of solution. After dehydration through a graded ethanol series, the tissues were immersed twice (15 min each) in propylene oxide and embedded in an

Epon type mixture prior to polymerization at 60°C for five days. After polymerization, semithin sections (0.25 μm) were cut and contrasted with a mixture of Azure II and methylene blue. Ultrathin silver sections were collected on Formvar-coated copper grids and stained with 2% uranyl acetate for 30 min and lead citrate for 10 min prior to examination with a JEOL 1010 or a Philips 301 transmission electron microscope operated at 80 kV. The remaining larger portion of the prostatic ventral lobe was fixed in 4% paraformaldehyde in 0.1 M phosphate buffer, pH 7.4, containing 2.5% sucrose, for 7 days followed by embedding in paraffin. Sections 3-5 μm thick were stained with hematoxylin and eosin (HE) and examined by light microscopy.

Volume of the prostatic ventral lobe

To estimate the gland volume the mass in g is multiplied by 0.95 [1] because the specific gravity of most parenchymal organs is about 1.05. By using a curve fitting procedure, a one-phase exponential decay curve expressing the change in gland weight was obtained, with the y-axis corresponding to the gland mass in mg and the x-axis being the number of days after castration. An equivalent equation expressed the relationship between the gland volume and the number of days post-castration.

Morphometric evaluation of the volume densities of the prostatic secretory epithelium (Vv_{epit}), glandular lumina (Vv_{glum}) and the space occupied by connective tissue and vessels (Vv_{con})

The morphometric procedures used were based on those described by Gundersen *et al.* [10], Aherne and Dunnill [1] and Carneiro and Sesso [7]. Prior to estimating the volume of a given structural component, the area or volume fraction, more commonly referred to as area (Aa) or volume density (Vv) of the component, was assessed using point counting volumetry. The numbers of points scored was sufficient to keep the operational error below 0.05 [10]. The sequence of morphometric parameters determined was as follows. Initially, we obtained the volume densities of the gland, the secretory epithelium (Vv_{epit}), the acinar lumina (Vv_{glum}) and the space between acini below the basal lamina of the secretory epithelium (Vv_{con}). This region of the gland includes the smooth muscle cells around the acini, the connective tissue and vessels. The glandular volume (μm^3) and gland weight were used to calculate the volume of the secretory epithelium (v_{epit}) for each gland on the various days after orchiectomy. The Vv_{epit}, Vv_{glum} and Vv_{con} were determined using HE-stained paraffin sections since these provided a larger area for examination than the semithin sections of tissue embedded in plastic resin.

The data obtained were corrected, as indicated in the Results, to express the same degree of histological shrinkage as seen in tissue processed for electron microscopy. To obtain the volume densities, 10-40 randomly selected histological fields were counted, using a x40 objective and a x8 Kpl ocular (Zeiss) containing a regularly spaced graticule of 100 points. The number of hits over the secretory epithelium, the glandular lumina and the interacinar space was scored. The volume densities of the secretory epithelium in the prostate (Vv_{epit}) was determined as the number of hits over the epithelium ÷ hits over the epithelium and the remainder of the gland. The hits over the epithelium included macrophages that had infiltrated through the epithelial basal lamina and were located in the basal region of the epithelium. The Vv_{glum} was determined as the number of hits over the acinar lumina ÷ total number of hits over the gland, i.e., the secretory epithelial and interacinar space (which includes vessels and connective tissue) plus the glandular lumina. The Vv_{con} corresponded to the number of hits over the interacinar spaces ÷ total number of hits over the gland. The epithelial volume (V_{epit}) was calculated as $V_{epit} = Vv_{epit} \bullet V_g$ (volume of the prostatic ventral lobe, in μm^3) (see Fig. 2).

Volume of the average secretory epithelial cell and of the secretory epithelium, and the number of secretory epithelial cells on successive experimental days

The mean nuclear volume of the prostatic epithelial nuclei (v_n) in castrated and non-castrated rats was obtained using the formula $v_n = L^3 \bullet \pi/3$ [11], where L is the length (in μm) of the intercepts obtained by the nuclear profiles formed with the parallel lines of the particular test system presented by the authors**.** The volume densities of the epithelial cell cytoplasm and nuclei (Vv_c and Vv_n) were obtained by point counts of calibrated prints with magnifications of x5,000 (2,000 x 2.5) and x4,125 (550 x 7.5). For each gland, at least ten random micrographs were measured. The Vv_n and Vv_c were obtained by counting the hits over nuclei and the cytoplasm. Vv_c was calculated as the number of hits over the cytoplasm ÷ the total number of hits over

the cell. The volume density of the nucleus (Vv_n) was calculated as 1 - Vv_c. The mean volume of the epithelial cells (v_e) was obtained from v_n and Vv_n, assuming that Vv_e is 1, such that
$v_e \bullet v_e = v_n \div Vv_n \bullet (v_c)$.

Number of epithelial cells and volume of the secretory epithelium

The number of epithelial cells was obtained by dividing the volume of the secretory epithelium (v_{se}) by the volume of the average epithelial cell (v_e), i.e., $v_{se} \div v_e$ = number of epithelial cells. The volume of the secretory epithelium was calculated as the product of the gland volume multiplied by the corrected volume density of the secretory epithelium in the gland, i.e., the volume density obtained in HE-stained paraffin sections multiplied by 1.49.

Total surface area of the main membrane-bound organelles of secretory epithelial cells

To determine the morphometric parameters of the cytoplasmic organelles, the test system proposed by Gundersen *et al.* [10], which consists of sets of regularly spaced segments, was applied to micrographs of the cytoplasm magnified x20,000 (8,000 x 2.5) and x31,500 (4,200 x 7.5). The number of hits (H) over the cytoplasmic matrix and organelles was counted, and the number of intersections (C) involving segments of the test system and the outer membrane of organelles was also scored.

The generic volume densities (Vv_i) and respective volumes (v_i) of cytoplasmic compartments such as the rough endoplasmic reticulum (RER), smooth endoplasmic reticulum (SER), Golgi apparatus (Golgi), mitochondria (Mit), various sized vesicles (Ves) and other structures were calculated from electron micrographs magnified x20,000 and x31,500, using the relationship $v_i = Vv_i \bullet v_c$, where v_i is the volume of a given compartment and v_c is the cytoplasmic volume, already determined from the average volume of the epithelial cell. At least ten electron micrographs were measured for each gland.

The membrane surface area of epithelial cell organelles (TS**)** was obtained using the formula $s/v = 4C \div L \bullet H$, where s/v is the surface-to-volume ratio of the organelle, i.e., the surface area (in μm^2) that 1 μm^3 of the organelle exposes to the cytoplasmic matrix, C is the number of intersections, H is the number of hits over the compartment or organelle, and L is the length of the lines (in μm) of the test system at a given magnification. To obtain the total surface area of the organelle (TS_{org}, μm^2), the organelle volume v_i was multiplied by s/v so that $TS_{org} = v_i \bullet s/v$. The sum of all the TS_{org} of the measured organelles yielded the total measured surface area of the membranes of an average epithelial cell (TS) on a given day of the experiment. The total measured surface area of the membranes of the secretory epithelium (TSE) was obtained by multiplying the TS by the corresponding number of epithelial cells, i.e., TSE = TS • number of cells.

Estimation of the total volume of intraepithelial dense bodies in the prostatic ventral lobe of castrated rats

The volume densities of the intraepithelial dense bodies (Vv_{db}), intraepithelial macrophages (Vv_m) and intramacrophage dense bodies (Vv_{dbm}) were calculated using 10-40 micrographs per gland at a magnification of 5,000 and 4,125. The method of Gundersen *et al.* [10] described above was used to count the hits over the intraepithelial dense bodies and over all of the other epithelial components above the basal lamina. In this method, Vv_{edb} corresponded to hits over epthelial dense bodies ÷ total hits over the epithelium, Vv_m corresponded to hits over macrophages ÷ total hits over macrophages and over the epithelium, and Vv_{mdb} corresponded to hits over macrophage dense bodies ÷ total hits counted (hits over macrophage dense bodies plus hits over the remaining portions of macrophages). The volume of all dense bodies (v_{totedb}) within the epithelia (intraepithelial and intramacrophage) was obtained by summing all of the respective volumes. The volume of the epithelial dense bodies (v_{edb}) was calculated as the epithelial volume (v_{epit}) on a given experimental day multiplied by the volume densities of the intraepithelial dense bodies (Vv_{edb}). Similarly, the volume of macrophages (v_m) on a given experimental day was calculated from the secretory epithelium volume (v_{epit}) and the volume densities of epithelial macrophages (Vv_m), i.e., $v_m = v_{epit} \bullet Vv_m$. The volume of macrophage dense bodies (v_{mdb}) was estimated as $v_m \bullet Vv_{mdb}$ (the volume density of macrophage dense bodies).

Estimation of the total surface area of membranes compacted in dense bodies (TS_{db})

The total membrane surface area that could be compacted in a dense body (TS_{db}) was estimated using an imaginary model of concentric spheres

(see Figs. 11, 13 and 14) in which it was assumed that the most external sphere had a volume of 1 μm^3. The formula used was $v_s = 4 \div 3\pi R^3$, where the radius R was 0.62 μm. The surface area of the spheres was obtained using the formula $s_s = 4\pi R^2$. The TS_{db} was calculated as the sum of the s_i of all concentric, adherent spheres at 0.005 μm intervals. This distance corresponded approximately to the thickness of the endoplasmic reticulum membrane. The total surface area of these juxtaposed concentric spheres in a volume of 1 μm^3 was 142 μm^2. The total membrane surface area compacted in epithelial dense bodies (TS_{totdb}) was obtained by multiplying the total volume of dense bodies in the epithelia (V_{totdb}) by 142. This estimate was based on images of juxtaposed unit membranes as shown in Figs. 14-16. These images preceded the last characterizable stage of dense body formation in which the bodies were stucturally less homogeneous and dense. Since in this last stage a membrane area greater than 142 μm^2 can be compressed into a volume of 1 μm^3, the membrane surface area present in the dense bodies was probably underestimated.

Measurement of the shrinkage of the prostatic ventral lobe and rat liver fragments after fixation and embedding in paraffin

Fresh organ fragments from three adult rats were sliced and then measured to the nearest millimeter. The fragments were fixed in buffered 4% paraformaldehyde for 48 h and embedded in paraffin, after which magnified images of stained sections were compared with the corresponding images of fresh tissue. For each rat, 1-2 fragments were measured to yield 6 and 5 fragments for the prostate and liver, respectively.

Estimation of the number of cells released to the glandular lumina

The number of cells released to the glandular lumina was determined by considering the glandular volume to be a cube. The number of microscopical fields of a given area that could fit in all the sections of this cube was then estimated. The total number of cells per gland was obtained by counting the apoptotic cells found in the acinar lumen per field in a representative sample. For this evaluation, 3-μm-thick HE-stained paraffin sections from the glands of two groups of rats, each with three animals castrated 4 and 5 days previously, were used. In each gland, at least ten microscopic fields were captured using a x20 objective and an Axiocamera with the associated Axiovision program from Zeiss. Each field in the monitor screen occupied an area of 19 x 15 cm that corresponded to a calibrated magnification of 351 x 10^3 μm^2. In each field, the cells lying in the acinar lumen were scored; most of these cells were apoptotic.

Characterization of apoptotic cells by the TUNEL reaction and by transmission electronmicroscopy.

Two-micrometer-thick paraffin sections from the glands of control rats and from rats that had been castrated for 1-10 days were processed for the TUNEL reaction using a commercial *in situ* cell death detection POD kit, according to the manufacturer´s instructions (Boehringer Mannheim, 1998). In this test, apoptotic nuclei were seen as a brown precipitate formed by a final peroxidase-DAB-H_2O_2 reaction.

Apoptosis was also recognized, under the transmission electron microscope, by the cell acquisition of the typical pattern of chromatin condensation. The detection of the apoptotic nuclear phenotype is recognized as the best procedure to identify this type of programmed cell death [23].

Histochemical reaction to identify macrophages

Two-micrometer-thick paraffin sections from control rats and rats that had been castrated for 1-10 days were processed to assess the presence of monocytes and macrophages based on immunodetection with an antibody (ED1; SEROTEC) that detects a protein present in lysosomal membranes. ED_1 is analogous to the human protein CD68 [8,9]. This antigen was detected as suggested by the manufacturer. The primary antibody against rat macrophage ED_1 (diluted 1/40) was incubated overnight at 4°C in a humid chamber and, after washing, a secondary antibody (rabbit anti-mouse antibody conjugated to biotin and diluted 1/500) was added for 30 min. This incubation was followed by a further wash and the addition of a third antibody conjugated with streptavidin-peroxidase (diluted 1/200) for 60 min. The two last steps were done in an humid chamber at 37°C. Addition of the substrate DAB with hydrogen peroxide resulted in a golden brown color when ED_1 was detected.

Statistical methods

The results were expressed as the mean ± S.E.M. Curve fitting procedures were done using a package

of programs from GraphPad Prism v. 4.00 for Windows (GraphPad Software, San Diego, CA, USA; www.graphpad.com). In most cases, the best fits for the x-y regression between the days after castration (x) and the morphometric parameter analyzed (y) were provided by a one-phase exponential decay curve of the type Y = Span*exp (-K*X) + Plateau, where K is a rate constant and the half life is 0.69/K, and a second degree polynomial equation of $Y = A + BX + CX^2$. In one case, a third degree polynomial equation provided the best fit to the x-y data. From these analyses, the coefficient of determination (r^2) and the F value for the regression of y against x were obtained. A value of $p<0.05$ indicated significance.

RESULTS

Qualitative results

The secretory epithelial cells of control and castrated rats were arranged as a layer of elongated columnar cells resting on a basal lamina that was generally in contact with the underlying smooth muscle cells (Fig. 1). Extremely well-developed rough endoplasmic reticulum (RER), Golgi apparatus and apically located secretory granules were observed. Macrophage-like cell profiles were rare and consistently small in controls (M in Fig. 1). A considerable number of dense bodies and a few lipofucsin-like bodies were normal components of the cytoplasm. By day 2 after castration, there was a noticeable increase in the number of intraepithelial dense bodies (Figs. 2 and 3) and a modest increase in the number of lipofucsin-like granules. Many of the dense bodies occurred close to or within the intercellular space in the basal region of epithelial cells (Figs. 3 and 4). Fig. 4 shows the engulfment of a dense body by a cytoplasmic projection from a macrophage. Apoptotic bodies within the cytoplasm of macrophages were much more frequent than the presence of apoptotic epithelial secretory cells, or of apoptotic bodies inside epithelial cells (Fig. 5). Occasionally, there was localized (Fig. 5) or generalized (Fig. 18) cytoplasmic lysis in secretory epithelial cells. The incidence of apoptosis and infiltration of intraepithelial macrophages peaked 4-6 days after castration (Fig. 6). In the glands of all castrated rats, a variable number of apoptotic epithelial cells or apoptotic bodies derived from epithelial cells was seen in the enlarged, basally located macrophages (Figs. 6-11). Figure 12 shows the concentric intracytoplasmic whorls of membranous material in an epithelial cell. Such formations tended to become compacted into dense bodies and, in some cases, were extruded to the intercellular space (Fig. 4) where they were ultimately engulfed by slender interepithelial macrophage projections (Figs. 3 and 4). The compaction of membrane-like material resulted in the formation of myelin-like profiles with membrane-like sheets arranged concentrically (Figs. 12 and 13). The apoptotic bodies within macrophages often showed a spectral arrangement of membranes derived from epithelial secretory cells. In a very early stage of formation, when an apoptotic body was engulfed by a macrophage, the membrane-bound organelles of the secretory cells resembled those of non-apoptotic epithelial cells. These membranes become naked, devoid of ribosomes, and showed a progressively more compacted, concentric arrangement that assumed the appearance of a dense body. Numerous sequential images suggested that most of the dense bodies found within macrophages (Figs 8-11) derived from a final compression in which membrane-like profiles appeared to be only tightly juxtaposed, e.g., Figs. 14-16. In an early stage of formation, the entire mass of the dense body consisted of tightly adherent unit membranes. In some cases, this arrangement was clearly visible (arrows in Fig. 17) while in others there was an accumulation of clear, tiny, circular dots that represented clear regions of the unit membrane occupied by the fatty acid chains of membrane phospholipids. Epithelial cells generally contained a greater overall amount of dense bodies than macrophages.

The lumina of the acini from castrated rats exhibited a variable number of apoptotic cells (Figs. 18-21). Under the electron microscope, rarely, dead cells of an yet undetermined nature may be seen (DC in Fig. 18) bordering the lumen. The vast majority of the luminar cells examined with the transmission electron microscope (Fig. 19) or in semithin sections (Figs. 21 and 22) are apoptotic. In H. E.-stained paraffin sections from castrated rats it is not rare to observe lumina devoid of dead cells. At the base of the bordering epithelium the macrophages appear as voluminous clear spaces with dense granules which correspond to phagocytized apoptotic bodies (Fig. 20).

TUNEL reaction and histochemical characterization of macrophages

All of the apoptotic bodies engulfed by macrophages reacted strongly in the TUNEL reaction. Considerably fewer nuclei from secretory epithelial cells

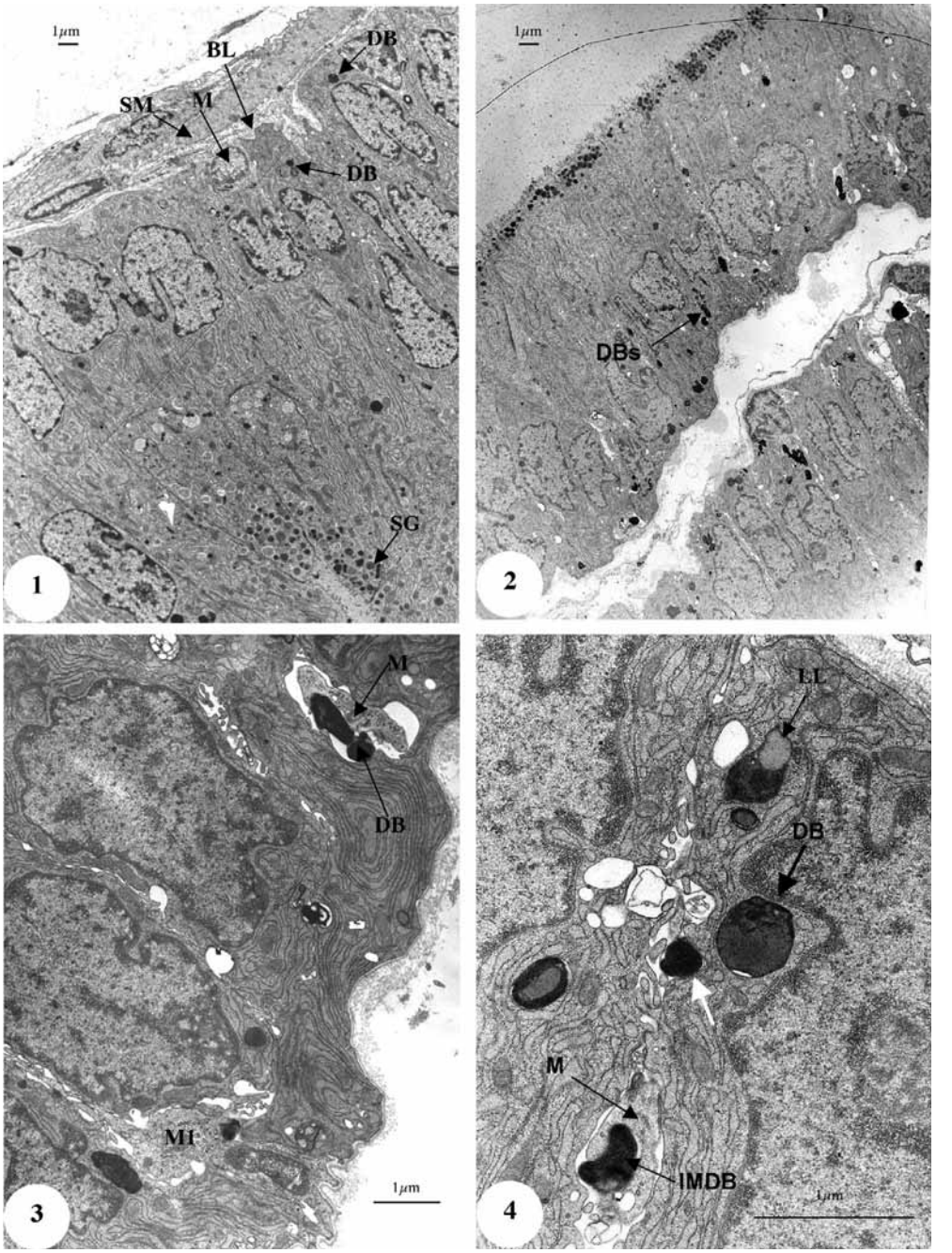

Figure 1. Prostatic secretory epithelium of a non-castrated (control) adult rat. Note the secretory granules **(SG)** located at the apex of large epithelial cells. Even at this low magnification, some intraepithelial dense bodies **(DB)** and an unactivated intraepithelial macrophage with its limited cytoplasm **(M)** can be seen. **BL** - basal lamina, **SMC** - smooth muscle cell. Bar = 1 μm.

Figures 2–4. Secretory epithelium two days after castration. Figure 3 is an enlarged view of a section of Figure 2. The density of intraepithelial and intercellularly located dense bodies **(DB)** is greater in these cells than in the corresponding control cells in Figure 1. The upper and lower regions of Figures. 3 and 4, respectively, show dense bodies being engulfed by cytoplasmic prolongations of macrophages **(M).** Various intraepithelial dense bodies **(DB)** are very close to the intercellular space, with one of them having already entered this space (**DB,** white arrow in Fig. 4). **IMDB** - intramacrophage dense body, **LL** - lipofucsin-like dense body, **MI** - cytoplasm of a basally located macrophage. Bars = 1 μm.

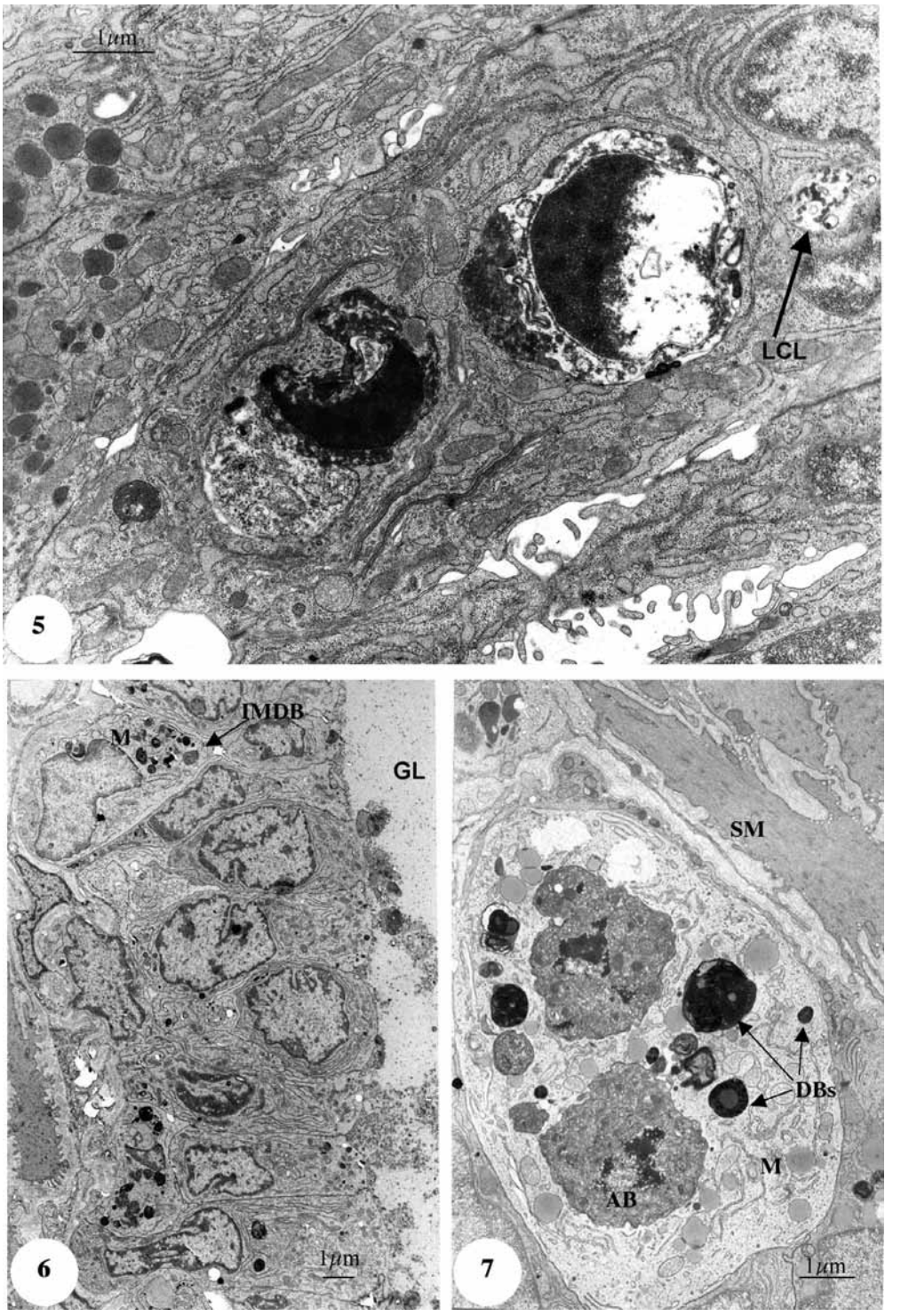

Figure 5. Two apoptotic bodies engulfed by a secretory epithelial cell in prostatic tissue two days after castration. **Arrow** indicates localized cytoplasmic lysis **(LCL)**. Bar = 1 μm.
Figure 6. Epithelial cell atrophy and an increase in the size of intraepithelial macrophages (**M**) six days after castration. Note the numerous dense bodies in these macrophages. **GL** - glandular lumen, **IMDB** - intraepithelial macrophage dense bodies. Bar = 1 μm.

also reacted. The incidence of TUNEL-positive cells with reacting apoptotic nuclei in epithelial secretory cells and in apoptotic bodies in the macrophage cytoplasm increased progressively from the second to the sixth day post-castration, with a peak between days 3 and 5. This pattern has been found to be so consistent in all of the glands from castrated rats that we now use sections obtained from the prostatic ventral lobe four days after castration as a control when other cell types are studied with the TUNEL reaction. The TUNEL reaction may, however, give positive results in necrotic cells.

As expected, the antibody ED_1 invariably reacted with the cells lying above the basal lamina at the base of the secretory epithelium and which contained engulfed bodies in their large cytoplasm.

Quantitative results

Glandular mass and volume

A curve fitting procedure furnished the following one-phase exponential decay curves (A and B in Table 1) to express the relationships observed: $y = 356.1\ e^{-0.15x} - 58.89$ where y = mass of the gland

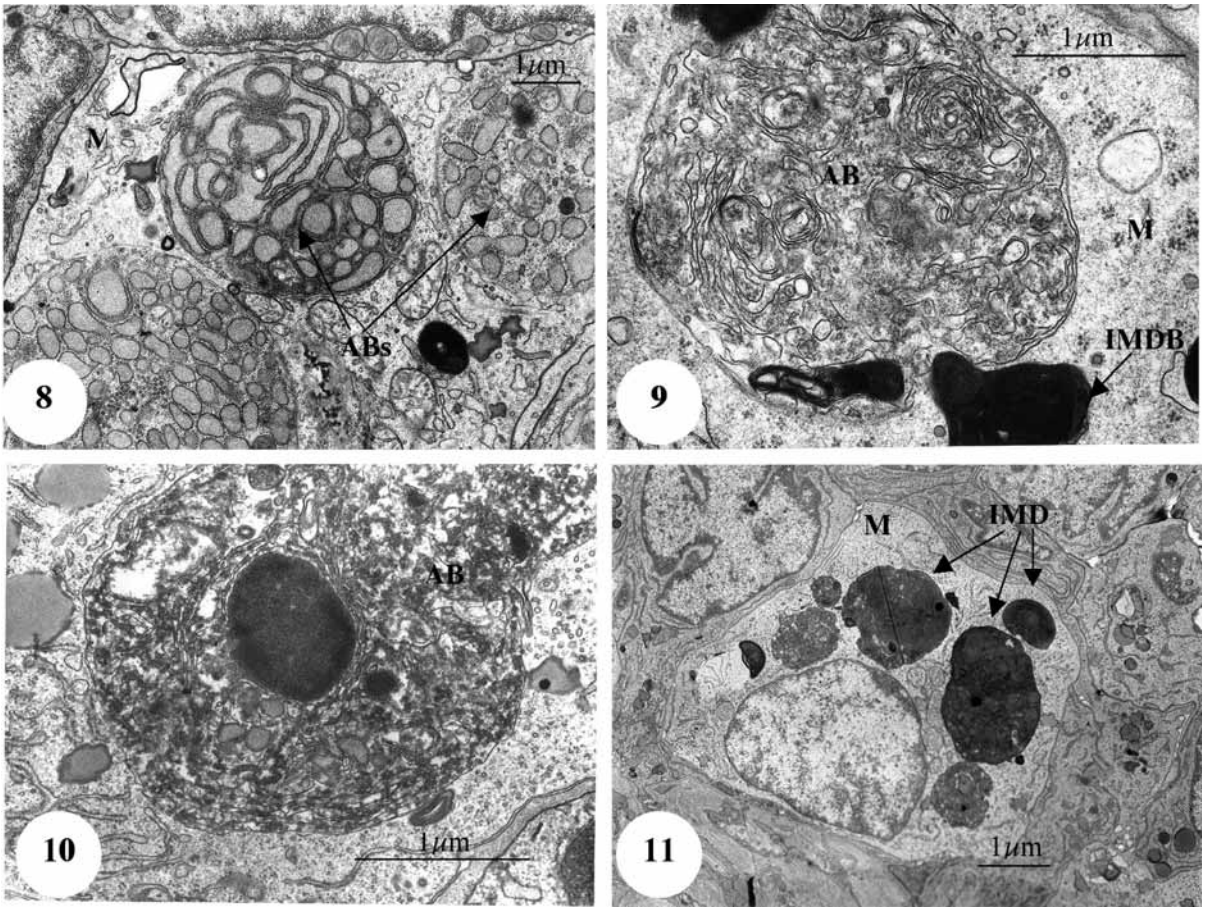

Figures 7-11. Successive structural changes in apoptotic bodies in the enlarged cytoplasm of macrophages **(M)** located close to the basal lamina of the epithelium four days after castration. Figure 7 shows various stages of the intramacrophage processing of material derived from apoptotic secretory epithelial cells. It is unclear whether the two large profiles indicated by **AB** represent whole apoptotic cells or apoptotic bodies derived from them. Various stages of compaction of dense bodies **(DB)** are shown. Figure 8 shows three circular profiles of apoptotic bodies derived from secretory epithelial cells. The variably good structural preservation of the RER membranes in these bodies indicates that they were recently been engulfed by the macrophage. Figures 9 and 10 show the inside of large apoptotic bodies (**AB**), with the ER being devoid (Fig. 9) or partially devoid of ribosomes (Fig. 10). These membranes are apparently in the process of compaction and may assume various configurations, including that of circular whorls (Fig. 9). In this figure, an apparently early formed intramacrophage dense body (**IMDB**) is indicated by an arrow at the periphery of the apoptotic body. The IMDB in Fig. 11 represent more advanced stages in the evolution of apoptotic bodies. Bars = 1 μm.

on day x, and y = 0.33 $e^{-0.15x}$- 0.05 where y = volume of the gland on day x (Fig. 23). The relative position of the points representing the mass or volume of control or castrated rats sacrificed on successive days after castration is the same and the shapes of the curves representing the evolution of these parameters are identical.

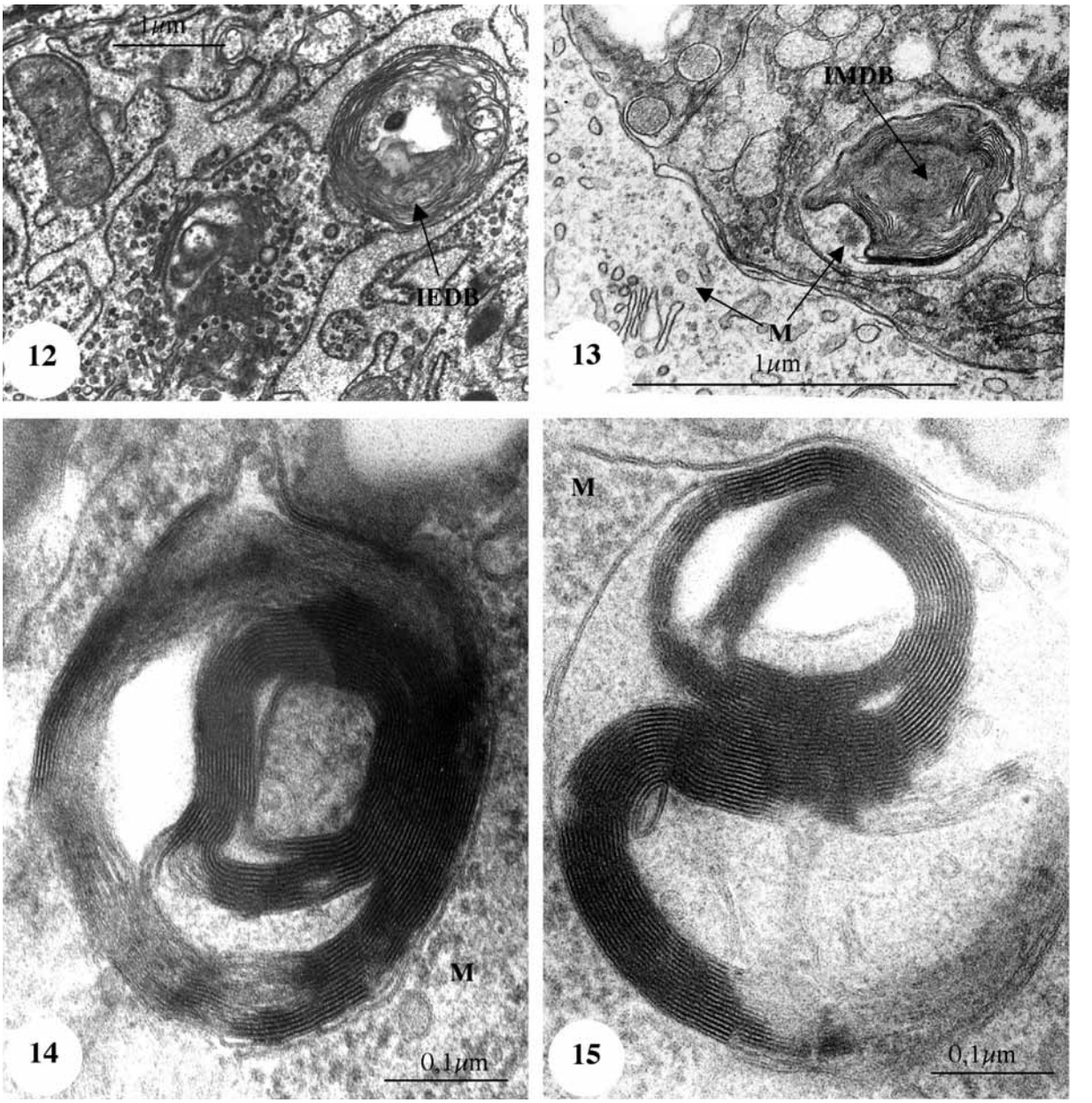

Figure 12. Cytoplasm of a secretory epithelial cell four days after castration showing an intraepithelial membranous whorl (**IEDB, arrow**) in the process of formation and apparently connected to the RER. Bar = 1 μm.

Figure 13. A stage in the formation of a dense body in an apoptotic body previously engulfed by a macrophage (**M**), the cytoplasm of which is indicated by arrows. The dense body (**IMDB**) is formed by concentric, membrane-like structures. Bar = 1 μm.

Figures 14-15. These two figures show that the dense body membranes are arranged similarly to those of myelinated nerves in which the basic structure of the unit membrane is a clear central band with a dense band on each side. These unit membranes are tightly adherent and probably in the process of forming a more voluminous, compact mass of cell membrane-derived material. **M** - macrophage cytoplasm. Bars = 0.1 μm.

The number of rats for each day after castration varied from 2 to 11. The half-life was 4.55 days and the r^2 was 0.679 ($p<0.01$) with 53 degrees of freedom. Day zero (0) refers to parameters obtained from non-castrated (control) rats. Based on the curves obtained nine days after castration, the gland fresh weight and volume diminished from 297 mg or 2.82 x 10^{11} μm^3 on day zero to 30 mg or 2.85 x 10^{10} μm^3 on the ninth day (A and B in Table 1), a decrase of approximately 90% compared to control rats.

Volume densities of the secretory epithelium, interacinar spaces and glandular lumina in the prostatic ventral lobe of glands embedded in paraffin

The progressive reduction in gland fresh weight and volume after castration had a half-life of 4.55 days. The decline in the volume density of the secretory epithelium (Vv_{epit}) in HE-stained paraffin sections was faster. This parameter halved every 1.69 days (C in Table 1). The volume of the secretory epithelium in paraffin imbedded glands was $V_{epitpar} = Vv_{epitpar} \bullet V_g$, where V_g is the gland volume. The volume densities of the epithelium ($Vv_{epitpar}$) were 0.40 on day zero, 0.34 at 12 h and 0.129 on day 9. An exponential one-phase exponential decay curve was chosen to analyze the changes in epithelial volume ($V_{epitpar}$). The processed volumes of the secretory epithelium from glands fixed in formalin and embedded in paraffin (data not included in Table 1) were 1.39 x $10^{11}\mu m^3$ on day zero, 1.05 x 10^{11} μm^3 after 12 h, 8.29 x 10^{10} μm^3 on day 1, 5.17 x 10^{10} μm^3 on day 2, 3.50 x 10^{10} μm^3 on day 3, 2.49 x 10^{10} μm^3 on day 4 and 1.30 x 10^{10} μm^3 on day 9. The increase in the Vvs of the interacinar space, which consists of connective tissue (Vv_{con}) and associated vessels, and the parallel decrease in the size of the acinar lumina (Vv_{glum}) on

Figure 16. The three intramacrophage apoptotic bodies shown in this figure are in progressively more advanced stages of processing their contents. An early stage is shown at the upper left. The profile on the right shows a few membranes with adherent ribosomes, with most of the remaining membranes being devoid of these organelles. Most of the dense profile close to the center has a myelin-like configuration. **M** - macrophage cytoplasm. Bar = 0.1 μm.

the days following castration, were expressed by second degree equations and are shown in D and E of Table 1. By day 9, the Vv_{con} was 2.5-fold greater than the control values while the Vv_{glum} declined to 40% of the value of control glands.

Comparison of secretory epithelial cell shrinkage in the prostatic ventral lobe after fixation and embedding in paraffin or Epon-like plastic resin

Organ fragments fixed in formalin and embedded in paraffin or fixed in glutaraldehyde-reduced osmium and embedded in an Epon-like plastic resin undergo different degrees of tissue shrinkage. Whereas in HE-stained, paraffin embedded sections the epithelial cells from control glands occupied 0.370-0.420 of the gland volume, the shrinkage seen in control glands fixed in glutaraldehyde-reduced osmium and embedded in Epon-like resin was significantly lower (0.552-0.662). To equate the shrinkage of epithelial cells seen in paraffin sections to that seen in TEM we multiplied the data obtained in the former sections by 1.49. Hence, all epithelial volumes (V_{epit}) derived from HE-stained sections was multiplied by 1.49 (see Material and Methods). These data are shown in Fig. 24 and in F in Table 1. Based on this correction, the volume of the secretory epithelium in non-castrated rats is $2.07 \times 10^{11} \mu m^3$ (F in Table 1). Every 1.23 days, the processed volume of the secretory epithelium corrected as described above was halved. By 12 h after castration, this volume was 1.56×10^{11} μm^3 and, by days 4 and 9 post-castration, represented 18% and 4% of the average volume found in the controls.

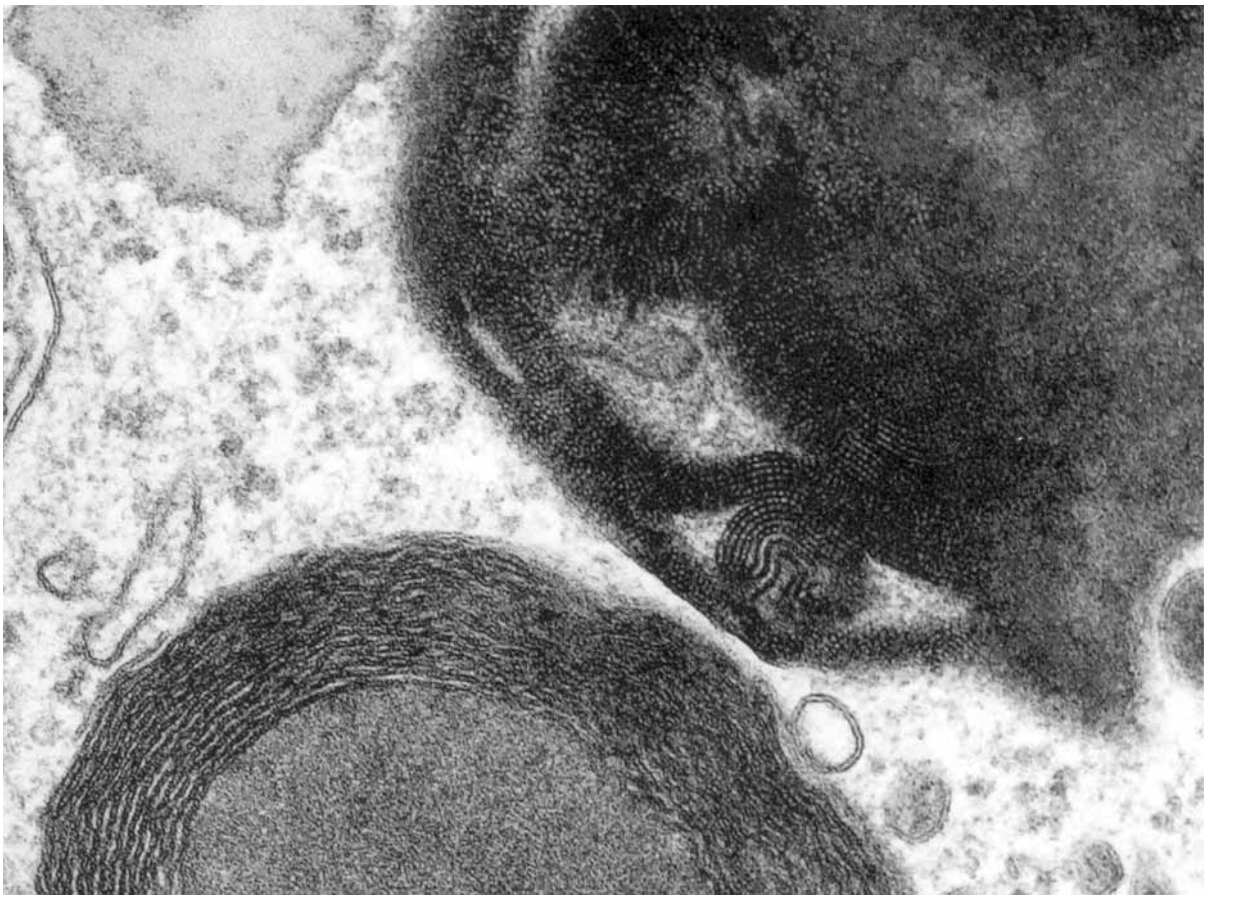

Figure 17. Macrophage from a rat four days after castration showing a dense body with a myelin-like arrangement at the cell periphery. The myelin-like arrangement of the membranous elements forming the dense body at the center and upper right is indicated by **arrows**. **M** - macrophage cytoplasm. Bar = 0.1 μm.

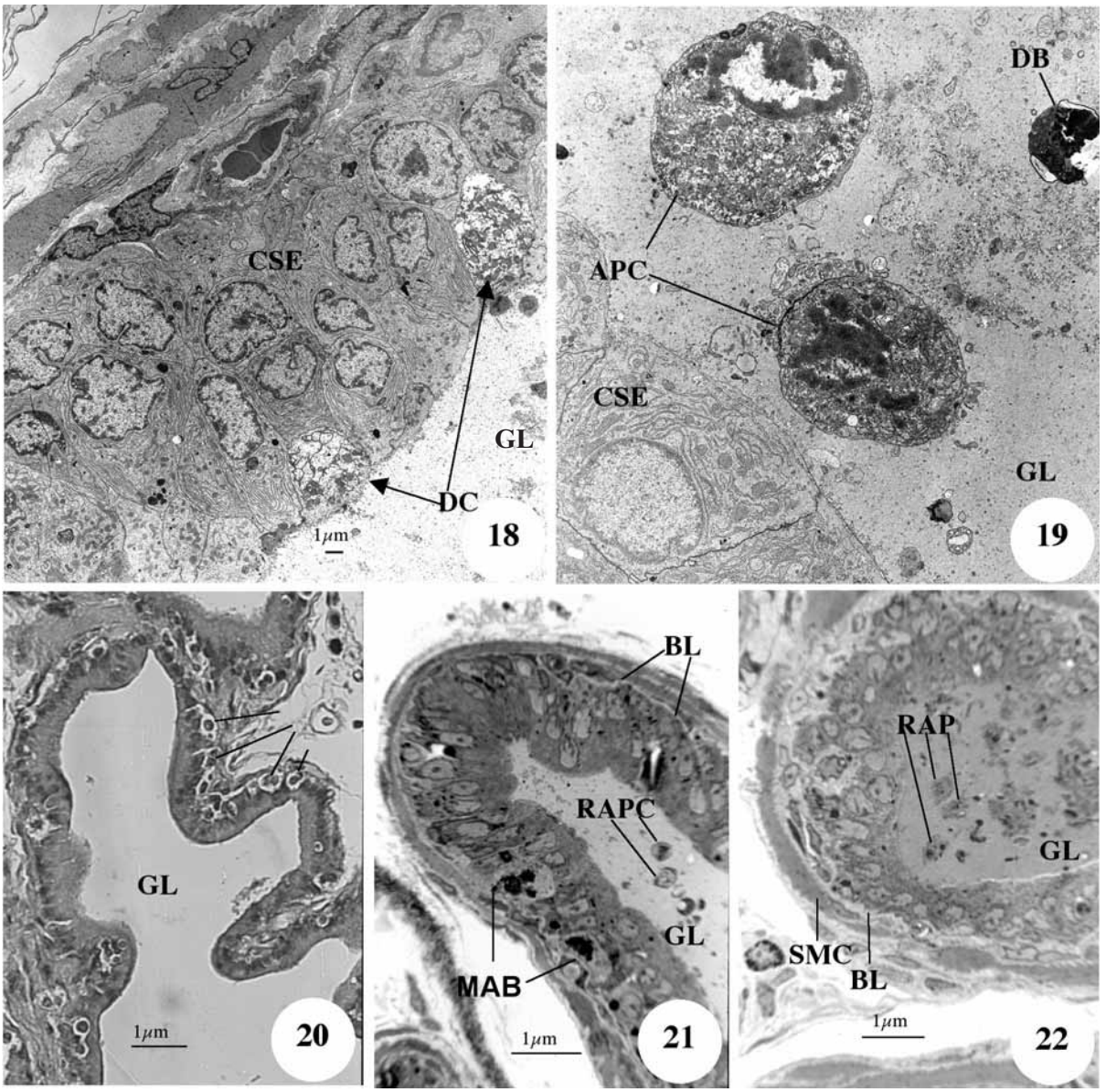

Figures 18-19. Cells of the secretory epithelium (**CSE**) and glandular lumen (**GL**) four days after castration. The two dead cells (**DC**) in Figure. 18 have lost their normal fine structure. The lysed cytoplasm permeating the organelles is structureless and clear. Figure. 19 shows two apoptotic secretory epithelial cells free in the glandular lumen. **DB** - luminar dense body. **APC** – apoptotic cell death. Bars = 1 μm.

Figures 20-22. Paraffin sections stained with HE (Fig. 20) and semithin plastic resin sections stained with methylene blue and azure A (Figs. 21 and 22) from glands four days after castration. An uncommonly high density of vacuolated, intraepithelial macrophages (**MAB**) is shown in Figure. 20. Large dense apoptotic bodies are shown in Figure 21. In Figures. 21 and 22, remnants of apoptotic cells (**RAPC**) are shown in the glandular lumen (**GL**). **BL** - basal lamina, **SMC** - smooth muscle cells. Bars = 1 μm.

Decrease in the total surface area of cytoplasmic membrane from the secretory epithelium of the prostatic ventral lobe following castration

To calculate this parameter, it was necessary to determine the average volume of atrophying secretory epithelial cells. Based on the declining exponential curve shown in G of Table 1, the average volumes of the secretory epithelial cells in control rats and 12 h and 1, 2, 3, 4 and 9 days after castration were 1070, 970, 883, 760, 684, 632 and 551 μm^3, respectively. The quotients of the volume of the secretory epithelium in the gland and the corresponding volumes of the secretory cells post-castration furnished the number of epithelial cells. Based on the curve $y = 1.909\ e.^{-239x} - 0.04534 \times 10^8$ (H in Table 1 and Fig. 25), the number of cells declined from 1.86×10^8 to 1.645×10^8 at 12 h after castration to only 10% of the number in control glands by day 9 post-castration.

Total measured surface area of cytoplasmic membranes in epithelial cells

The total measured surface area of the membranes of one epithelial cell (TS) represents the sum of the membrane surface area of each membrane-bound compartment of the cytoplasm [RER, SER, Golgi apparatus, mitochondria, various sized vesicles and other structures]. The surface areas obtained from an exponential one-phase decay curve (I in Table 1 and Fig. 26) were 6750, 5190, 5150, 3970, 3150, 2500 and 1120 μm^2 in control rats and in glands from castrated rats after 12 h and 1, 2, 3, 4 and 9 days, respectively. The individual values of the average membrane surface area multiplied by the respective number of epithelial cells gives the total surface area of cytoplasmic membranes of the secretory epithelium. These results are shown in J of Table 1 and in Fig. 27. The reduction in the total surface area of the secretory epithelium seen nine days after castration was the most pronounced of all of the morphometric parameters studied. These values halved every 1.15 days. Based on the one-phase decay exponential curve, in the initial 12 h after castration the membrane surface area declined 26% compared to the control values (9.6×10^{11} μm^2 and 12.9×10^{11} μm^2, respectively). By the ninth day after castration, the total membrane surface area in the secretory epithelium corresponded to ~3% (0.43×10^{11} μm^2) of the control value.

Assessment of the potential capacity of dense bodies to store compressed membranes during the castration-induced demise of secretory epithelial cells

Dense bodies in macrophages

In control rats, macrophages represented 0.06% of the volume of the secretory epithelium. By days 1 and 4 after castration, these values corresponded to 1.39% and 3.78% and represented increases of 23- and 63-fold above the control (L in Table 1). The net volume of the macrophages increased until the fourth day post-castration but declined thereafter until day 9 (M in Table 1), in parallel with the decline in the volume of the secretory epithelium during this period. The changes in the volume densities of dense bodies in macrophages are shown in N in Table 1 and in Fig 28. The volume density of intraepithelial macrophages in the secretory epithelium increased markedly soon after castration. In control rats, the few macrophages present were small and contained no dense bodies; rather, these cells began to appear only 24 h after castration. Between days 1 and 9, the volume densities of the intramacrophage dense bodies rose 18-fold. Based on these data, the volume of the intramacrophage dense bodies was estimated as shown in O of Table 1. This volume increased until the fourth day after castration and decreased thereafter.

Overall, the intramacrophage dense body volumes represented a relatively small fraction of the intraepithelial dense body volume. Comparison of the data in O and P of Table 1 shows that the volumes of the intramacrophage dense bodies on post-castration days 1, 2, 3, 4 and 9 accounted for 0.05%, 0.08%, 1%, 2% and 4% of the corresponding intraepithelial dense body volumes, respectively. To convert the intramacrophage dense body volume into a possible reservoir for membrane surface area, the percentages obtained above were multiplied by 142. If the values of membrane surface area that can be potentially stored in epithelial dense bodies and the corresponding membrane surface area storable in macrophage dense bodies are summed**,** the curve expressing the total membrane area surface that can be stored in the dense bodies of epithelial cells and macrophages does not differ significantly from $y = 2.218 + 1.472x - 0.1838x^2$ shown in Q of Table 1. The low values for macrophage dense bodies were insufficient to overcame the data scatter of intraepithelial dense bodies, thus minimizing or annulling the expression of the effects of the addition.

Membrane surface area that can be potentially stored in dense bodies of the secretory epithelium

The volume of intraepithelial dense bodies (v_{edb}) can be obtained for each gland by multiplying the values of Vv_{edb} (K in Table 1) by the corresponding volume of the secretory epithelium (v_{se}) (F in Table 1) for a given day of the experiment, i.e., $v_{ebd} = Vv_{edb} \bullet v_{se}$. Based on the third degree polynomial equation shown in Table 1, the v_{edb} (P in Table 1 and Fig. 29) in non-castrated rats was 1.23 x 10^8 μm^3 compared to 2.39 x 10^8 μm^3, 12 h after castration, and 3.31-, 4.09-, 3.98-, 2.69- and 0.455 x 10^8 μm^3 on days 1, 2, 3, 4 and 9 after castration, respectively. When the individual data for dense body volume in the secretory epithelium were multiplied by 142, the membrane surface area storable in a myelin-like arrangement inside a dense body was obtained (Q in Table 1). On day 1 after castration, the estimated surface area was 2.22 x 10^{10} μm^2 (an increase of 58% relative to the controls) and by day 4 the increase was 232% above the control value. The percentage of membrane surface area storable in epithelial dense bodies on successive days after castration relative to the total membrane surface area existing in the secretory epithelium on the same day is shown in J and R of Table 1 and in Fig. 30). The amount of membranes that could be stored in the dense bodies of control epithelial cells corresponded to 1.5% of the total measured membrane surface area of the epithelium. This percentage rose to 25% on day 4 after castration and to 47.6% on day 9.

Volumetric shrinkage of fresh glandular tissue after fixation and embedding in paraffin

The linear retraction of the six paraffin-embedded fragments of ventral lobe from three control adult rats was 26.9 ± 6.5; a similar degree of retraction (27.4 ± 3.47) was seen in five liver fragments from the same animals. The prostatic ventral lobe showed a 39.1% reduction in volume relative to fresh glandular tissue. By using the fresh glandular volume shown in Fig. 23 and in B in Table 1, the processed glandular volumes on days 4 and 5 post-castration were calculated to be 1.28 • 0.3908 = 0.5002 x 10^{11} μm^3 and 1.01 • 0.3908 = 0.3947 x 10^{11} μm^3, respectively.

Estimation of the number of secretory epithelial cells released into the acinar lumina 4 and 5 days after castration

To determine how the total number of cells released into the acinar lumina on the fourth day after castration was related to the decline in the number of secretory epithelial cells (F in Table 1) between days 3 and 4, we estimated how many microscopical fields could be counted in the processed glands on the fourth and fifth days after castration. On day 4, this volume was 50.02 x 10^9 μm^3. The cubic root of 50.02 x 10^9 μm^3 is the side of a cube 3,685 μm in length. This cube will furnish 1228 sections 3 μm thick (=3685÷3). Each section has an area of 13,579,225 μm^2 (=3685^2). This value multiplied by the number of sections gives 16,675,288,300 μm^2 and corresponds to the total area to be scanned in the gland. The number of microscopic fields is 16,675,288,300 μm^2 ÷ 351,000 μm^2 = 47,508. The number of secretory epithelial cells declined by 20 x 10^6 from day 3 to day 4 (F in Table 1). If these cells are equally distributed in the glands of castrated rats after four days then we would expect to find 20 x 10^6 ÷ 47,508 = 421 cells per field. Counts in 20 randomly chosen fields from glands 4 and 5 days after castration (n = 3 each) yielded 10.9 ± 2.01 cells and 4.8 ± 0.96 cells in the acinar lumen, respectively ($p<0.03$ for the difference between these means). The average of 10.9 cells in the acinar lumen per microscopic field four days after castration corresponded to 47,508 • 10.9 =517,837 cells. This number represents 2.6% (517,837 ÷ 20 x 10^6) of the dead cells if the count reflects the number of cells released during the previous 24 h. However, if the cells counted in the lumen showed disintegration or had lysed nuclei (the latter were used to count the number of dead cells), then in a 4-h period the percentage of dead cells would correspond to approximately 16% of all of the epithelial cells that had died in the previous 24 h. By the fifth day after castration, the processed gland volume of 39.47 x 10^9 μm^3 was considered to be a cube with a lateral dimension of 3,405 μm. This cube will furnish 1135 sections 3 μm thick (=3405 ÷ 3), with each section having an area of 11,594,025 μm^2 (= $3405)^2$ and a total area for all sections of 13,159,218,375 μm^2. This area corresponds to 37,491 microscopical fields, each with 351,000 μm^2. Based on the data in Fig. 25 and H in Table 1 on days 4 and 5, the number of secretory epithelial cells was 0.68 x 10^8 and 0.053 x 10^8, a reduction of 15 x 10^6. Five days after castration, the number of intraluminal cells per microscopical field was 4.8 cells, which corresponded to 4.8 • 37,491 = 179,957 cells and represented 1.2% (179,957 ÷ 150,000) of the number of cells that disappeared from the gland

Table 1. Morphometric data from regression curves.

Measured parameters		Days	y	Measured parameters		Days	y
Gland mass (mg)		0	$297x10^{11}$	Gland volume (μm^3)		0	2.82×10^{11}
$y = 356.1.e^{-0.15x} - 58.89 \times 10^{11}$		1	$246 x10^{11}$	$y= 0.33.e^{-0.15x} - 0.05 \times 10^{11}$		1	2.33×10^{11}
Half-life = 4.55 days (d)	**A**	2	$203 x10^{11}$	Half-life = 4.55 d	**B**	2	1.92×10^{11}
n = 56		3	$166 x10^{11}$	n = 56		3	1.57×10^{11}
53 degrees of freedom		4	$134 x10^{11}$	53 degrees of freedom		4	1.27×10^{11}
r^2 =0.679(P<0.01).		9	$30 x10^{11}$	$r^2 = 0.679$ (P<0.01).		9	2.85×10^{10}
Vvs of the glandular secretory epithelia		0	0.396	Vvs of the interacinar space of the ventral lobe		0	0.291
$y=0.3529.e^{-0.4379x} + 1.58$		1	0.305	$Y =0.2909+0.09154x - 0.00468x^2$		1	0.378
Half-life = 1.69 d	**C**	2	0.245	n = 16	**D**	2	0.455
n = 17		3	0.207	13 degrees of freedom		3	0.522
14 degrees of freedom		4	0.181	$r^2 = 0.860$ (P<0.01)		4	0.581
$r^2 = 0.869$ (P<0.01).		9	0.129			9	0.736
Vvs of the intraacinar lumina of the ventral lobe		0	0.309	Secretory epithelia volumes (μm^3) with		0	2.07×10^{11}
$y = 0.3090-0.01959x-0.0001159x2$		1	0.289	correction factor of 1.49		1	1.22×10^{11}
n = 16	**E**	2	0.269	$y = 1.881.e^{-0.562x}+1.226 \times 10^{i}$	**F**	2	0.795×10^{10}
13 Degrees of Freedom		3	0.250	Half-life = 1.23 d		3	0.535×10^{10}
$r^2 = 0.574$ (P<0.01).		4	0.229	n = 16		4	0.381×10^{10}
		9	0.123	13 degrees of freedom		9	0.085×10^{10}
				$r^2 = 0.860$ (P<0.01).			
Average epithelial cell volumes (μm^3)		0	1.07×10^3	Number of secretory epithelial cells x 10^8		0	$1,86 \times 10^8$
$y = 528.4e^{-0.47x}+552.9 \times 10^{i}$		1	8.83×10^2	$y = 1.909\ e^{-0.2394x} - 0.04534 \times 10^8$		1	1.465×10^8
Half-life = 1.45 d	**G**	2	7.60×10^2	Half-life = 2.90 d	**H**	2	1.13×10^8
n = 14		3	6.84×10^2	n = 16		3	0.88×10^8
11 d egrees of freedom		4	6.32×10^2	13 degrees of freedom		4	0.68×10^8
$r^2 = 0.655$ (P<0.01).		9	5.51×10^2	$r^2 = 0.932$ (P<0.01)		9	0.18×10^8
Total membrane surface area in an average		0	$6,75 \times 10^3$	Total membrane surface sreas		0	12.9×10^{11}
epithelial cell (μm^2)		1	5.15×10^3	in the epithelia (μm^2)		1	7.10×10^{11}
$y = 6043.e^{-0.29x} + 714 \times 10^3$	**I**	2	3.97×10^3	$y = 12.51.e^{-0.6041x} + 0.3760 \times 10^{11}$	**J**	2	4.10×10^{11}
Half-life = 2.311 d		3	3.15×10^3	Half-life = 1.147 d		3	2.4×10^{11}
n = 11		4	2.50×10^3	n = 16		4	1.5×10^{11}
8 degrees of freedom		9	1.12×10^3	14 degrees of freedom		9	0.43×10^{11}
$r^2 = 0.966$ (P<0.01).*				$r^2 = 0.956$ (P<0.01).			
Vvs of the secretory epithelial dense dodies		0	0.0013	Vvs of epithelial macrophages		0	0.0006
$y = 0.001253+0.001772x-0.0001403x^2$		1	0.0029	$y = 0.00069+0.01417x-0.001235x^2$		1	0.0139
n = 15	**K**	2	0.0042	n = 16	**L**	2	0.0245
13 degrees of freedom		3	0.00529	13 degrees of freedom		3	0.0322
$r^2 = 0.423$ (P<0.01).		4	0.0061	$r^2 = 0.695$ (P<0.01).		4	0.0378
		9	0.0058			9	0.0281
Volumes of intraepithelial macrophages (μm^3)		0	3.49×10^8	Vvs of the intramacrophage dense bodies		0	0
$y = 0.3490+0.6482x-0.07368x^2$		1	9.37×10^8	$y=0.00007906+0.000515x+0.00005618x^2$		1	0.000515
n = 16	**M**	2	1.36×10^9	n = 16	**N**	2	0.001172
13 degrees of freedom		3	1.63×10^9	13 degrees of freedom		3	0.001940
$r^2 = 0.646$ (P<0.01).		4	1.76×10^9	$r^2 = 0.622$ (P<0.01).		4	0.002870
		9	2.15×10^8			9	0.009106
Volumes of intramacrophage dense bodies (μm^3		0	0	Volumes of total intraepithelial dense bodies		0	1.23×10^8
x 10^6)		1	$1.67x10^6$	(μm^3)		1	3.31×10^8
$y = -0.5024 + 2.406x-0.2370x^2 x10^6$		2	$3.36 x10^6$	$y = 1.238+2.729x-0.7499x^2+0.04856x^3 X10^8$		2	4.09×10^8
n = 16	**O**	3	$4.58 x10^6$	n = 16	**P**	3	3.98×10^8
13 degrees of freedom		4	$5.33 x10^6$	13 degrees of freedom		4	2.69×10^8
$r^2 = 0.311$ (P<0.05)		9	$1.90 x10^6$	$r^2 = 0.756$(P<0.01).		9	0.455×10^8
Maximal capacity of dense bodies to store the		0	$2.22 x10^{10}$	Percentage of the total (y) epithelial measured		0	0.015
measured epithelial membrane surface area (μm^2)		1	$3.50 x10^{10}$	membrane areas stored in dense bodies on the		1	0.078
$y = 2.218 + 1.472x - 0.1838x^2 x 10^{10}$		2	$4.43 x10^{10}$	indicated days		2	0.138
n = 16		3	$4.95 x10^{10}$	$y = 0.01539+0.06453x-0.001480x^2$		3	0.196
13 degrees of freedom	**Q**	4	$5.17 x10^{10}$	n = 16	**R**	4	0.250
$r^2 = 0.677$ (P<0.01)		9	$0.58 x10^{10}$	13 degrees of freedom		9	0.476
				$r^2 = 0.596$ (P<0.01)			

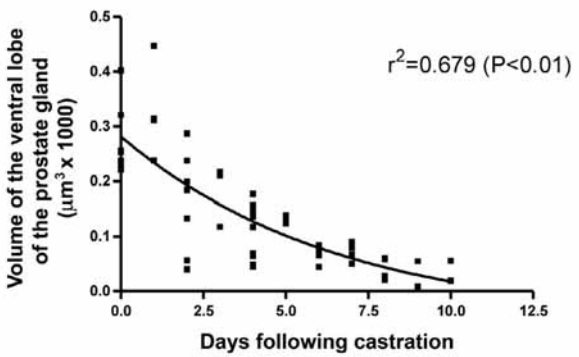

Figure 23

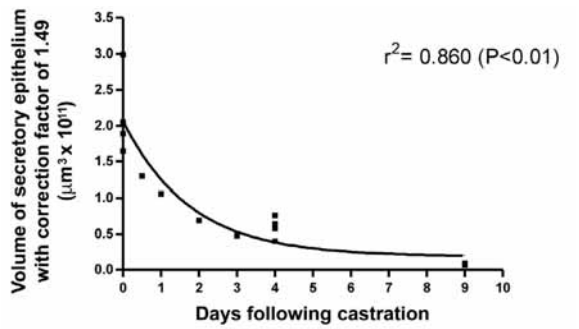

Figure 24

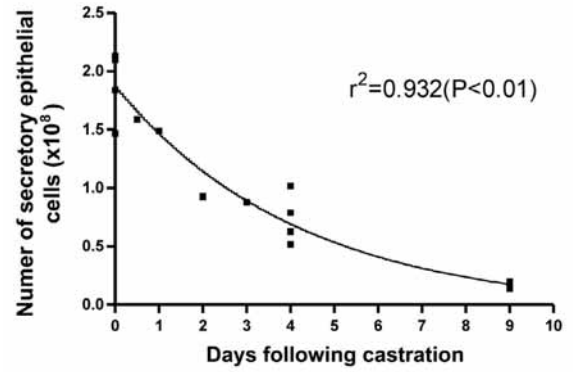

Figure 25

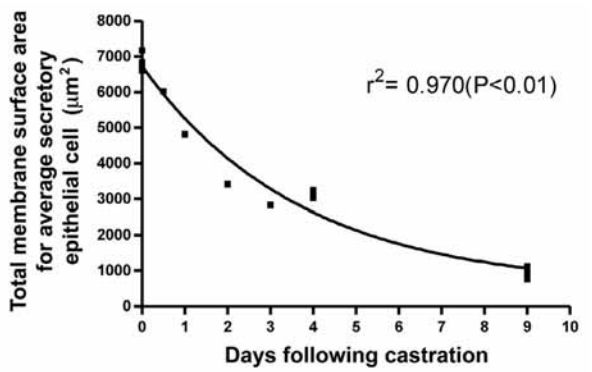

Figure 26

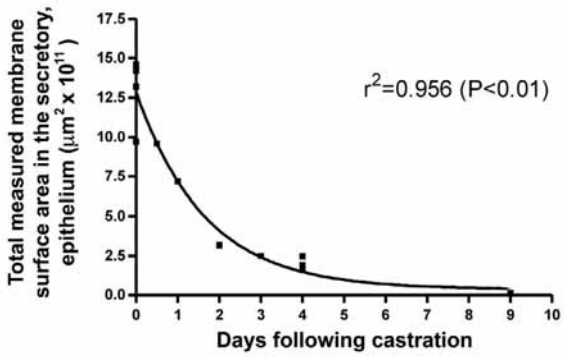

Figure 27

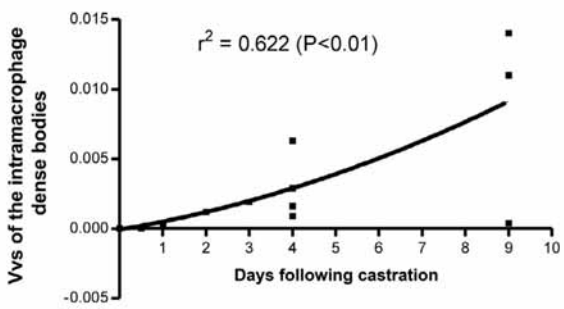

Figure 28

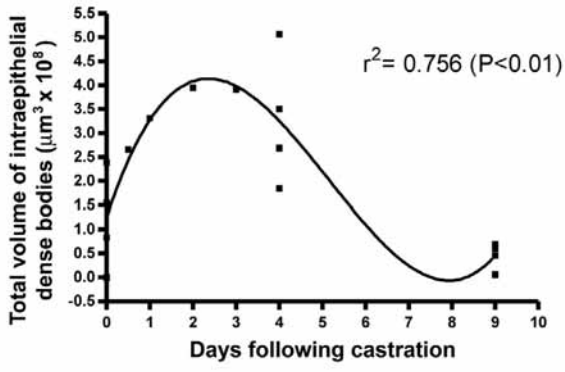

Figure 29

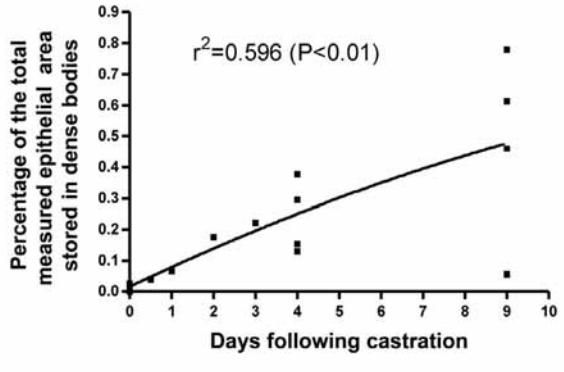

Figure 30

between days 4 and 5. Acceptance of this value of 1.2% implies that all of the cells counted remained in the lumina throughout the last 24 h period.

DISCUSSION

The results described here show that castration reduces the gland wet weight, increases the incidence of apoptosis in secretory epithelial cells and alters the fine structure in atrophying cells. These findings generally agree with the results of other studies [4,5,17,19-22].

A loss of wet weight was seen within three days of castration, with a decrease of 75% after seven days [4]. By the seventh day post-castration, there occurred a ~80% reduction in the gland fresh weight. These effects were more pronounced than in the other lobes of the rat prostate. The dorsal and lateral lobes responded more slowly and less dramatically to castration, with their wet weights decreasing significantly only by the seventh day; there was a 45-50% loss by 15 days after castration [4].

Alterations in mitochondrial membranes are characterized by rupture of the outer membrane at a focal point, with the inner membrane escaping via a gap to form a large bulge [20]. This description coincides with the morphology of the mitochondrial permeability transition seen in numerous types of apoptotic cells [21] and initially described in mitochondria of apoptotic hepatocytes [2].

Based on TUNEL labeling in cells of the prostatic ventral lobe, Kwong *et al.* [20] reported a progressive increase in the frequency of apoptosis that peaked three days after castration. We also observed maximal TUNEL reactions 3-5 days after castration. Our results were similar to those of Kyprianou and Isaacs [19] who observed a peak incidence of apoptosis on the fourth day after orchiectomy, with 80% of the prostatic cells being lost by the tenth day post-castration.

Some of our observations regarding the role of macrophages in capturing portions of the cytoplasm of apoptotic secretory epithelial cells have been published elsewhere [20]. When the epithelial cell is in advanced apoptosis, its cytoplasm is concentrated in spherical bodies with remnants of organelles in its interior, especially in cisternae of RER arranged concentrically. These spherical bodies are phagocytized by macrophages or are eventually detached from the epithelium and released into the acinar lumen [20].

The morphometric data shown in A to R of Table 1 and in Figs. 23-30 provide relevant contributions to our knowledge about the rate of disappearance of cells in the secretory epithelium of the prostatic ventral lobe and of their constituent membranes. The morphological sequence of transformations that the membranes of secretory epithelial cells undergo in intramacrophage phagocytic bodies (Figs. 8-11, 16 and 17) also represent new contributions. These data confirm the idea that dense bodies represent an economical way of disposing of useless intracytoplasmic membranes. Spherical portions of secretory apoptotic cells in the cytoplasm of secretory epithelial cells and the presence of apoptotic bodies in macrophages were also described by Kwong *et al.* [20].

Intraepithelial dense bodies

The sequential changes in the concentrically arranged cytoplasmic membranes of secretory cells and the frequent occurrence of a myelin-like arrangement of these membranes in the apoptotic bodies of macrophages agreed with the view that these formations were precursors of the final stage of dense body formation. An analysis of how the increase in intraepithelial dense bodies relates to a concomitant decrease in the total membrane surface area of the secretory epithelium will be helpful at this point. Examination of Fig. 29 and P in Table 1 shows that the change in the total volume of the intraepithelial dense bodies is represented by a third degree polynomial equation, the only one to pass over the points representing 12 h and 1, 2 and 3 days after castration.

To determine the minimum amount of membrane surface area that can be stored in these dense bodies, the volumes must be multiplied by 142 (see Material and Methods). Comparing the data in J with those in P of Table 1 shows that between days 0 and 1, 1 and 2, 2 and 3, and 3 and 4 the total membrane surface area in the secretory epithelium decreased by 5.8, 3.0, 1.7 and 0.9 x 10^{11} μm^2, respectively. On days 0, 1, 2, 3 and 4, the respective total membrane surface areas that could be stored in epithelial dense bodies (obtained by multiplying the dense body volumes in P of Table 1 by 142) were 0.175, 0.470, 0.581, 0.565 and 0.382 x 10^{11} μm^2. As shown in Fig. 29, the curve increases up to two days after castration, indicating a net increase in the volume and in the corresponding surface area of storable membranes. These net increases were 0.470 – 0.175 x 10^{11} μm^2 = 0.295 x 10^{11} μm^2 and

$0.581 - 0.470 \times 10^{11}\ \mu m^2 = 0.111 \times 10^{11}\ \mu m^2$. These values represent 5.1% (0.295/5.8 = 0.051) and 3.7% (0.111/3.0 = 0.037) of the membrane surface areas that diminished in the secretory epithelium between post-castration days 0 and 1 and 1 and 2. These percentages are actually underestimations, one cause of which is the turnover of dense bodies of the secretory epithelium. In non-castrated rats, the epithelium contains a large number of dense bodies whereas these structures are very rare in intraepithelial macrophages. The presence of lipofucsin-like bodies in the epithelial cells of control and castrated rats indicates the occurrence of autophagocytosis in these cells.

These observations raise the possibility that these epithelial cells constantly renew part of their cytoplasm. This suggestion is supported by the results of Kwong *et al.* [20] in which the apoptotic index of secretory epithelial cells was 1% in the prostatic ventral lobe in non-castrated rats but reached 2.6% three days after castration. These apoptotic indices show that this secretory epithelium normally renews part of its cells. The dense bodies in epithelial cells may represent an aspect of this process.

Intramacrophage dense bodies

Although the infiltration of macrophages into the secretory epithelium caused by castration has an important role in forming dense bodies from engulfed apoptotic secretory epithelial cells, the net amount of such bodies compared to the dense bodies of the secretory epithelium is relatively small. Recently formed apoptotic bodies and various dense bodies are frequently seen in macrophages (Fig. 7), a finding that suggests the cells involved have been in operation for a relatively long time. Yet these images provide no clue as to the time that macrophage require to completely process the ingested apoptotic bodies. We do not even know if these intramacrophage bodies are ultimately dissolved. By 3-4 days after castration, the peak of the total volumes of intramacrophage dense bodies ($\sim 5 \times 10^6\ \mu m^3$) represented 1-2% of the volume of intraepithelial dense bodies ($\sim 4 \times 10^8\ \mu m^3$).

The roles of macrophage and secretory cell dense bodies in the homeostasis of tissue membranes can only be fully appreciated once the duration of these structures has been established. Fig. 28 and N in Table 1 provide some information on the time that macrophages spend in the intraepithelial region. The volume densities of the intramacrophage dense bodies increase from day 1 to day 9 post-castration. This progressive increase in the proportion of cellular area occupied by dense bodies means that newly formed dense bodies were added to pre-existing dense bodies during this post-castration interval. These macrophages were apparently incorporated into the epithelium from the beginning of the experiment but remained at the base of the epithelial cells.

It is unclear why the incidence of apoptotic cells in the secretory epithelium was lower in preparations stained by the TUNEL reaction and in those examined by TEM than that seen in intramacrophage apoptotic bodies. Considering that a large number of preparations was examined by TEM at various times after castration and that these observations covered large time intervals of time (hours), it is surprising that not a single image of macrophages in the process of engulfing the spheroidal portion of an apoptotic secretory epithelial cell was obtained. Perhaps the speed with which apoptotic epithelial cells are engulfed by macrophages makes the event difficult to document.

Disposal of dead epithelial cells via release into the acinar lumina

The number of secretory epithelial cells that died between days 3 and 4 and 4 and 5 was 20×10^6 and 15×10^6, respectively. In 20 randomly chosen microscopical fields of 351,000 μm^2 each in 3 μm thick paraffin sections from rats castrated 4 and 5 days previously, the number of luminal cells was 10.9 ± 2.01 and 4.8 ± 0.96, respectively. Assuming that these figures were representative of the number of cells found in the acinar lumina of all of the microscopical fields of the entire gland, it was estimated that luminar cells represented at least 2.6% and 1.2% of the number of secretory epithelial cells lost between days 3 and 4, and 4 and 5, respectively. Implicit in the estimation of these percentages is the unlikely possibility that the cells counted had been in the lumina for an entire 24 h period.

Final remarks regarding the role of dense bodies as depositories of useless membranes

We have stressed that a lack of knowledge about the length of time that intraepithelial and intramacrophage dense bodies spend in cells has meant that the role of these bodies as a reservoir for used membranes has generally been underestimated. Another frequent cause of underestimations is the use of a common factor to transform dense body volume into compacted membrane surface area. In the present

study, we estimated the potential storage capacity of dense bodies by multiplying their volumes by 142 based on a model in which the membranes were juxtaposed in a myelin-like configuration. These membranes may, however, be further compressed by an as yet undetermined amount. In this case, the factor required to obtain the actual area of compressed membranes will be greater than 142.

ACKNOWLEDGMENTS

The authors thank Maria M.T. Monteiro, Maria C. da Rocha, Maria C.S.L. Marcondes, Angel B.G. dos Santos, Regiani C. de Oliveira Resende and Gildásio V. Rocha of the Department of Pathology, Faculty of Medicine, University of São Paulo, for their technical support. Materials utilized in this work were partially derived from funding from FAPESP (Processos 00/06648-2 and 00/08891-1) and the CNPq (Processo 303329/2004-1)

REFERENCES

1. Aherne AW, Dunnill MS (1982) *Morphometry*. 1st edn. Edward Arnold: London.
2. Angermuller S, Kunstle G, Tiegs G (1998) Pre-apoptotic alterations in hepatocytes of TNFα-treated galactosamine-sensitized mice. *J. Histochem. Cytochem.* **46,** 1175-1183.
3. Banerjee PP, Banerjee S, Brown TR (2001) Increased androgen receptor expression correlates with development of age-dependent, lobe-specific spontaneous hyperplasia of the brown Norway rat prostate. *Endocrinology* **142,** 4066-4075.
4. Banerjee PP, Banerjee KIT, Tilly JL, Brown TR, Zirkin BR (1995) Lobe-specific apoptotic cell death in rat prostate after androgen ablation by castration. *Endocrinology* **136,** 4368-4376.
5. Brandes D (1966) The fine structure and histochemistry of prostatic gland in relation to sex hormones. *Int. Rev. Cytol.* **20,** 207-276.
6. Brandes D, Groth DP (1963) Functional ultrastructure of rat prostatic epithelium. *Natl. Cancer Inst. Monogr.* **12,** 47-62.
7. Carneiro SM, Sesso A (1987) Morphometric evaluation of zymogen granule membrane transfer to Golgi cisternae following exocytosis in pancreatic acinar cells from suckling newborn rats. *J. Submicrosc. Cytol.* **19,** 19-33.
8. Damoiseaux JGMC, Dopp EA, Calame W, Chao D, MacPherson GG, Dijkstra CD (1994) Rat macrophage lysosomal membrane antigen recognized by monoclonal antibody ED1. *Immunology* **83,** 140-147.
9. Dijkstra CD, Dopp EA, Joling P, Kraal G (1985) The heterogeneity of mononuclear phagocytes in lymphoid organs: distinct macrophage subpopulations in the rat recognized by monoclonal antibodies ED1, ED2 and ED3. *Immunology* **54,** 589-599.
10. Gundersen HJ, Bendtsen TF, Korbo L, Marcussen N, Moller A, Nielsen K, Nyengaard JR, Parkenberg B, Sorrensen FB, Vesterby A, West MJ (1988) Some new, simple and efficient stereological methods and their use in pathological research and diagnosis. *Acta Pathol. Microbiol. Immunol. Scand.* **96,** 379-394.
11. Gundersen HJ, Jensen EB (1985) Stereological estimation of the volume-weighted mean volume of arbitrary particles observed on random sections. *J. Microsc.* **138,** 127-142.
12. Harkin JC (1957) An electron microscopic study of the castration changes in the rat prostate. *Endocrinology* **60,** 185-199.
13. Hayashi N, Sugimura Y, Kawakamura J, Donjacour AA, Cunha GR (1991) Morphological and functional heterogeneity in the rat prostatic gland. *Biol. Reprod.* **45,** 308-321.
14. Helminen HJ, Ericsson JLE (1971) Ultrastructural studies on prostatic involution in the rat. Mechanism of autophagy in the epithelial cells, with special reference to the rough-surfaced endoplasmic reticulum. *J. Ultrastruct. Res.* **36,** 708-724.
15. Helminen HJ, Ericsson JLE, Arborg B (1972) Differing patterns of acid phosphatases and cathepsin D activities in the rat ventral prostate and during castration-induced prostatic involution. *Acta Endocrinol.* **69,** 747-761.
16. Jesik CJ, Holland JM, Lee C (1982) An anatomic and histologic study of the rat prostate. *Prostate* **3,** 81-97.
17. Kerr JFR, Searle J (1973) Deletion of cells by apoptosis during castration-induced involution of rat prostate. *Virchows Arch Abt. B. Zellpat.* **13,** 87-102.
18. Kiplesund KM, Halgunset J, Fjosne HE, Sunde A (1988) Light microscopic morphometric analysis of castration effects in the different lobes of the rat prostate. *Prostate* **13,** 221-232.
19. Kyprianou N, Isaacs J (1988) Activation of programmed cell death in the rat ventral prostate after castration. *Endocrinology* **122,** 552-562.
20. Kwong J, Choi HL, Huang Y, Chan FL (1999) Ultrastructural and biochemical observations on the early changes in apoptotic epithelial cells of the rat prostate induced by castration. *Cell Tissue Res.* 298, 123-136.
21. Sesso A, Marques M, Monteiro M, Schumacher R, Colquhoun A, Belizário J, Konno S, Felix T, Botelho L, Santos V, Silva G, Higuchi M, Kawakami J (2004) Morphology of mitochondrial permeability transition: morphometric volumetry in apoptotic cells. *Anat. Rec.* **281A,** 1337-1351.
22. Stiens R, Helpap B (1981) Regressive change in the rat prostate after castration. A study using histology, morphometrics and autoradiography with special reference to apoptosis. *Pathol. Res. Pract.* **172,** 73-87.
23. Yasuhara S, Zhu Y, Matsui T, Tipirneni N, Yasuhara Y, Kaneki M, Rosenzweig A, Martyn JA (2003) Comparison of COMET assay, electron microscopy and flow cytometry for detection of apoptosis. *J. Histochem. Cytochem.* **51,** 873-885.

Received: November 28, 2005
Accepted: January 6, 2005